

## Effect of controlling parameters on heat transfer during spray impingement cooling of steel plate

Purna C. Mishra, Santosh K. Nayak, Rajeswari Chaini, Durga P. Ghosh,  
Bibhuti B. Samantaray

<sup>1</sup> School of Mechanical Engineering, KIIT University, Bhubaneswar – 751024, Odisha, India

**Abstract:** - The heat transfer characteristics of air-water spray impingement cooling of stationary steel plate was experimentally investigated. Experiments were conducted on an electrically heated flat stationary steel plate of dimension 120 mm x 120 mm x 4 mm. The controlling parameters taken during the experiments were air-water pressures, water flow rate, nozzle tip to target distance and mass impingement density. The effects of the controlling parameters on the cooling rates were critically examined during spray impingement cooling. Air assisted DM water was used as the quenchant media in the work. The cooling rates were calculated from the time dependent temperature profiles were recorded by NI-cRIO DAS at the desired locations of the bottom surface of the plate embedded with K-type thermocouples. By using MS-EXCEL the effects of these cooling rate parameters were analysed. The results obtained in the study confirmed the higher efficiency of the spray cooling system and the cooling strategy was found advantageous over the conventional cooling methods in the present steel industries.

**Keywords:** - Heat transfer coefficient, Heat transfer enhancement, spray Impingement Cooling, Optimal cooling, Patternator.

### Nomenclature:

$\Delta T$	Measured temperature difference
$\Delta T^*$	Non-dimensional temperature difference
$T_c$	Temperature of cooling water
$T$	Time
$t^*$	Non-dimensional time
$l$	Length of the steel plate
$\alpha$	Coefficient of thermal expansion
CR	Cooling rate
CR*	Non-dimensional cooling rate
$d$	Hole diameter
$D$	Shower exit to surface distance
$K$	Thermal conductivity
lt	Liter
min	Minute
m	Meter
s	Second
$P_w$	Water Pressure

### I. INTRODUCTION

Spray Impingement cooling (SIC) is a very promising thermal management technique for high heat flux applications like Runout Table Cooling in Hot Strip Mill. Heat fluxes as high as 10 MW/m<sup>2</sup> with SIC has been reported by Selvam and Ponnappan, [1].

Several technologies [2–5] to increase the cooling rate in the ROT have been recently developed. Ultrafast cooling technology [2, 3] increases the conventional cooling rate of  $30\text{ }^{\circ}\text{C/s}$  to  $80\text{ }^{\circ}\text{C/s}$ , depending on the final thickness, to  $300\text{ }^{\circ}\text{C/s}$  on 4-mm-thick hot strip. An accelerated cooling technology [4, 5] having more than  $200\text{ }^{\circ}\text{C/s}$  on 3-mm thickness makes it possible to increase the strength of steel or to achieve the same level of strength with a low carbon equivalent design. These technologies use larger flow rates than conventional cooling methods (such as spray or water column cooling), basically. In the ultrafast cooling, total water flow is well known as  $17,000\text{ L/min m}^2$  [3] of cooling length. This corresponds to  $9200\text{ L/min m}^2$  assuming a 1.8-m width, [4] which is more than double the maximum flow rate for the conventional ROT cooling [3]. Bhattacharya et al., [6] reported that Ultra Fast Cooling (UFC) in Hot Strip Mill entails cooling rate of about  $300\text{ }^{\circ}\text{C/s}$ , which corresponds to heat transfer rate of  $4.37\text{ MW}$  for a 4 mm thick carbon steel strip. The cooling rate obtained was an order of magnitude higher than conventional laminar jet cooling.

As such, there is very less information about the method to achieve high strip cooling rate with SIC in open literature. Using air/ water spray impingement cooling instead of conventional laminar water jet impingement cooling might help to achieve the ultra-high strip cooling rate of SIC.

Investigations involving air and water flow rates and impact-water fluxes within ranges of practical interest to continuous casting (i.e., 5 to 10 g/s (i.e., 3.9 to 7.8 NL/s), 0.3 to 0.6 L/s, and 2 to 90 L/m<sup>2</sup> s, respectively) have shown that the droplet dynamics persist in having an important influence on impaction heat transfer [7-9].

In recent times, Ravikumar et al [10] tested the atomized spray cooling on a plate maintained at the initial surface temperature of  $900^{\circ}\text{C}$ . They concluded that air atomized cooling provides very high cooling rates which lead to produce high strength steels on ROT. Yu Hou et al.[11] experimentally studied on phase change spray cooling. A R22 pressure spray cooling system was designed and built. The system cooling performance was experimentally investigated with the nozzle inlet pressure in the range of 0.6 MPa to 1.0 MPa. Enhancement of cooling rate of an AISI 304 steel plate by air atomized spray cooling with different types of surfactant additives has been studied in the present work. The heat transfer during spray cooling was studied experimentally by Zhen Zhang et al.[12] on one flat and three enhanced surfaces using deionized water for flow rates from 22.2 L/h to 60.8 L/h, orifice-to-surface distances from 0.5 cm to 3.0 cm and spray inclination angles from  $0^{\circ}$  to  $45^{\circ}$ . J. Wendelstorf [13] was studied about the heat transfer for spray water cooling of clean surfaces using full cone nozzles ( $v_d=14\text{ m/s}$ ,  $d_d=350\text{ }\mu\text{m}$ ) in the parameter range  $V_s = 3\text{--}30\text{ kg/(m}^2\text{ s)}$  and surface temperatures between 200 and  $1100\text{ }^{\circ}\text{C}$  were investigated. An additional temperature dependency in the high temperature (Leidenfrost effect) was found. The stable film boiling regime shows an HTC decreasing with temperature difference for  $V_s > 10\text{ kg/(m}^2\text{ s)}$  and  $DT$  above  $\approx 800\text{ K}$ . The absolute accuracy of the HTC measurement was better than 11% in the film boiling regime.

## II. EXPERIMENTAL SET UP

Figure 1 shows the schematic of the experimental setup with details of its components used in the present work. The experimental setup was used to investigate quenching heat transfer with air/water sprays. The test piece consisted of an electrically heated steel sheet of dimension  $120 \times 120 \times 4\text{ mm}$ . A square base electrical coil-heater of 2.5 KW capacity was used to heat the plate to the desired temperature, upper side of which was cooled by the air/water spray being investigated. Three full cone air atomizing nozzles were used to generate the spray. The delivery water pressure from the pump was controlled by pressure regulator. The spray cooling test stand got regulated water and air from the pumping system. The nozzle water output was changed to various combinations of water pressure and air pressure to attain required flow rate of air-water mixture. A simple mechanical patternator was used to measure the local and average water impingement density. The local time-dependent surface temperature distribution was measured on the bottom side embedded with K-type thermocouples at desired locations. For each test four thermocouple data were obtained through the data acquisition system (cRIO) supplied by NI Systems Ltd. The obtained data were processed using LabVIEW software.

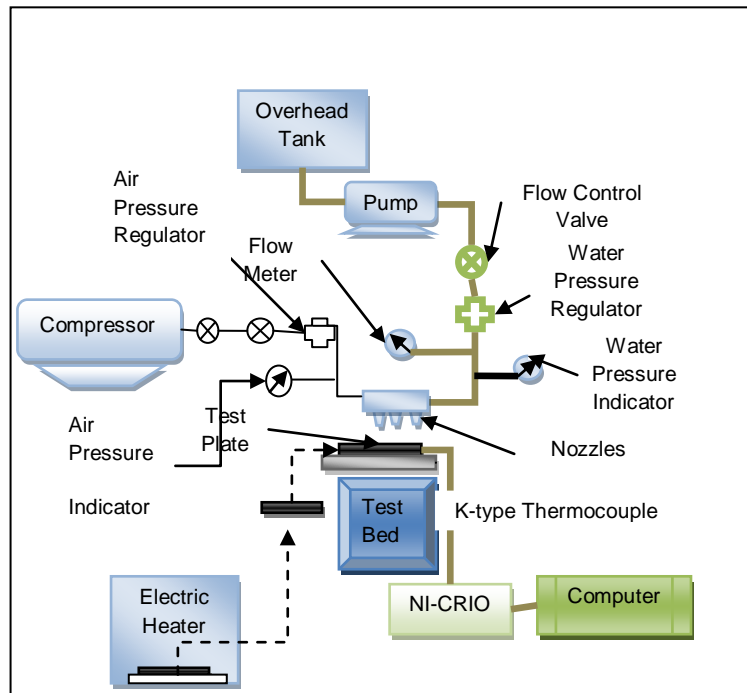


Figure- 1: Schematic Of The Experimental Setup

A sample of thermocouple arrangement on the plate is shown in the following.

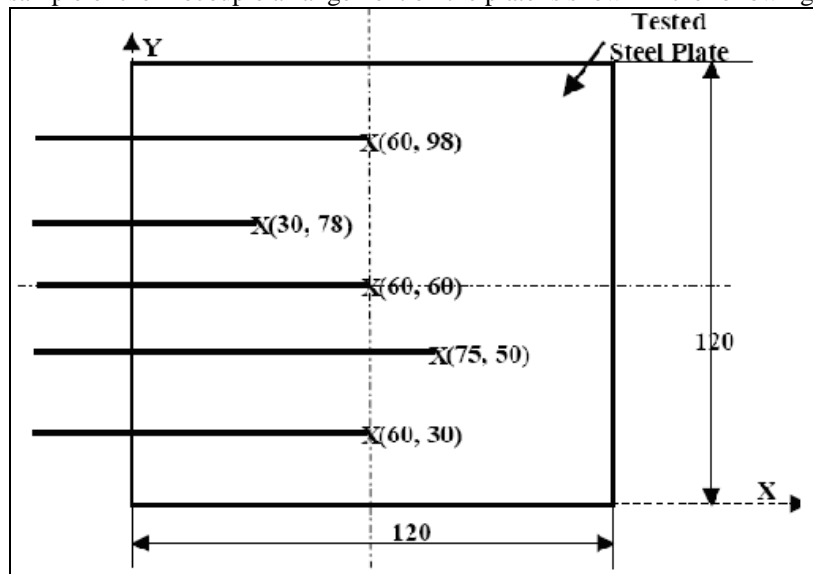


Figure 2. Sketch Of Thermocouple Installation Location

### III. EXPERIMENTAL PROCEDURE

The steel plate had to be heated to a temperature slightly higher than the test temperature because some amount of heat would be lost from the heated test plate during the transfer from heater to the test bed. Then this hot steel plate was taken out of the heater and positioned on the test bed (underneath the air atomizing nozzles). While the temperature of the steel plate dropped the required temperature, the spray was turned on and impinged on the hot plate surface. The spray was set at different combinations of air and water pressures. The air pressure ranged from 0.0 bar to 4.0 bar and water pressure varied from 2.0 bar to 4.0 bar. At each combinations of air and water pressure, the water flow rate was recorded directly by using the flow meter during spray impingement cooling. The real time data of temperature history of plate heating and cooling was recorded continuously by

using the NI cRIO DAQ system and supported LabVIEW software. The dimensionless initial temperature differences ( $\Delta T^*$ ) of test plate in these experiments were varied from 16.67 to 30. The nozzle to surface spacing was considered as fixed at 42 mm. In addition to the heat transfer measurement, the local impingement density at various air-water pressure combinations was measured by using the simple mechanical patternator. From the transient time-temperature data obtained in the experiments, the maximum dimensionless cooling rate was computed and recorded for further parametric analysis.

#### IV. RESULT AND DISCUSSION

Cooling rate is one of the important factors used to determine the rate of heat transfer during a cooling on a hot steel plate by water/air mixture spray cooling. The experimental data obtained concerning the rate of heat transfer has been presented to summarize the behavior of spray impingement cooling processes.

##### 4.1. Effect of the Injection Point and Cooling Curves:

The injection point has great influence on the cooling profile during spray impingement cooling of a flat steel plate. The non-dimensional temperature difference is computed as the ratio of measured temperature difference ( $\Delta T$ ) and cooling water temperature ( $T_c$ ), while the non-dimensional cooling time is obtained from Equation 1.

$$\Delta T^* = \frac{\Delta T}{T_c} \text{ and } t^* = \frac{l^2}{\alpha} \cdot t \quad 1$$

The possible influence of the injection point are shown in Figure 3 and figure 4, where the dimensionless plate surface temperature difference ( $\Delta T^*$ ) is plotted with respect to dimensionless cooling time ( $t^*$ ) for different air pressure and at water pressure of 3bar and 2.5 bar respectively. It is observed from Figure 4 that the central thermocouple shows an interesting cooling trend between dimensionless temperature difference ( $\Delta T^*$ ) and cooling time ( $t^*$ ) during air-water spray cooling. From the point of injection there is a rapid drop of temperature as the cooling time passing. At different values of air pressure the temperature difference profiles show different trends from which the contribution of air in the spray cooling can easily be identified. It is clear that at combined air and water pressures at 2.0 bar and 3.0 bar, the temperature distribution is sharp while at 3.5 bar air pressure and 3.0 bar water pressure, it is relatively flattened. This is due to the fact that with increase of air pressure to a higher value the atomisation also increases, but the water flow rate decreases, decreasing the heat transfer and the tiny water droplets evaporate before falling on the plate. Thus, the air-water pressure combination is to be optimized to achieve the optimal heat transfer rate, which is also evident from Figure 4. From Figure 4, the cooling effect is clearly understood for air-water mixed spray impingement cooling. In the absence of air (i.e.,  $P_A = 0.0$  bar), the convection process is only possible due to water and the dimensionless temperature difference profile greatly changes. It is due to the atomization.

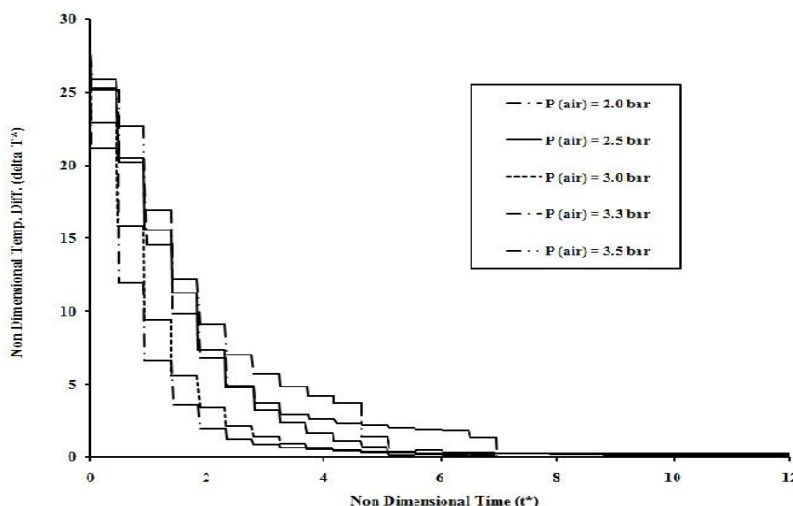


Figure3. Non Dimensional Temperature Difference ( $\Delta T^*$ ) Vs. Time ( $T^*$ ) At Different Air Pressures And 3.0 Bar Water Pressure.

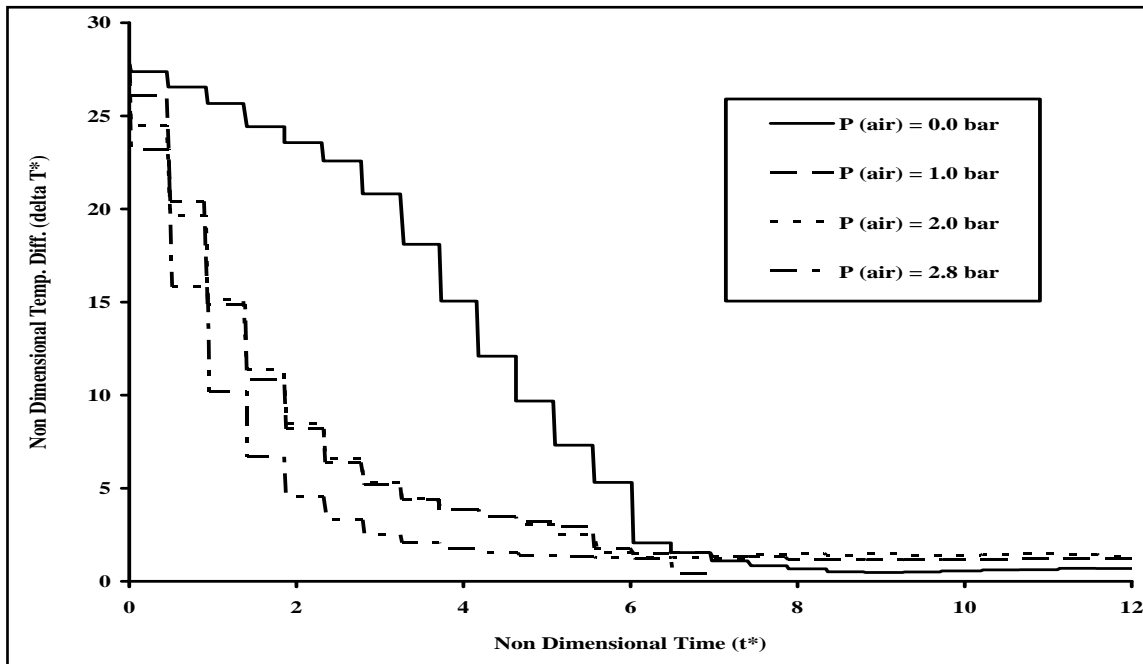


Figure 4: Non Dimensional Temperature Difference ( $\Delta T^*$ ) Vs. Time ( $T^*$ ) At Different Air Pressures And 2.5 Bar Water Pressure.

**4.2. Cooling Rate (CR):**

From the measured dimensionless time dependent temperature distribution curves at each thermocouple location, the corresponding maximum value of cooling rates were computed by taking the peak values of temperature and time and using Equation 2.

$$CR = \frac{T_2 - T_1}{t_2 - t_1}, \text{ } ^\circ C/Sec \tag{2}$$

Further, the cooling rate in Equation 2 is non-dimensionalized by using Equation 3.

$$CR^* = \left[ \frac{\Delta T^*}{t^*} \right] = \frac{l^2}{\alpha \cdot T_c} \left[ \frac{\Delta T}{t} \right] \tag{3}$$

The highest and lowest values of dimensionless cooling rate ( $CR^*$ ) obtained in the experiments were 13.65 and 5.89, respectively.

**4.3. Effect of Air/Water Pressure:**

Figure 5 shows the effect of air pressure on the dimensionless cooling rates achieved for different fixed water pressures. From Figure 5, it could be observed that the highest value of non dimensional cooling rate ( $CR^*$ ) obtained for the central thermocouple at the 1.0 bar air and 2.5 bar water pressure combination is 9.104, whereas the highest value of non dimensional cooling rate of central thermocouple at air and water pressure combination of 2.5 bar and 3.0 bar is 14.67. Experimental results reveal that the more is the air pressure, there is a significant change in the cooling rate at a fixed water pressure. Hence, mixing of air with water has a predominant role in enhancing the heat transfer rate from the steel plate surface during spray quenching.

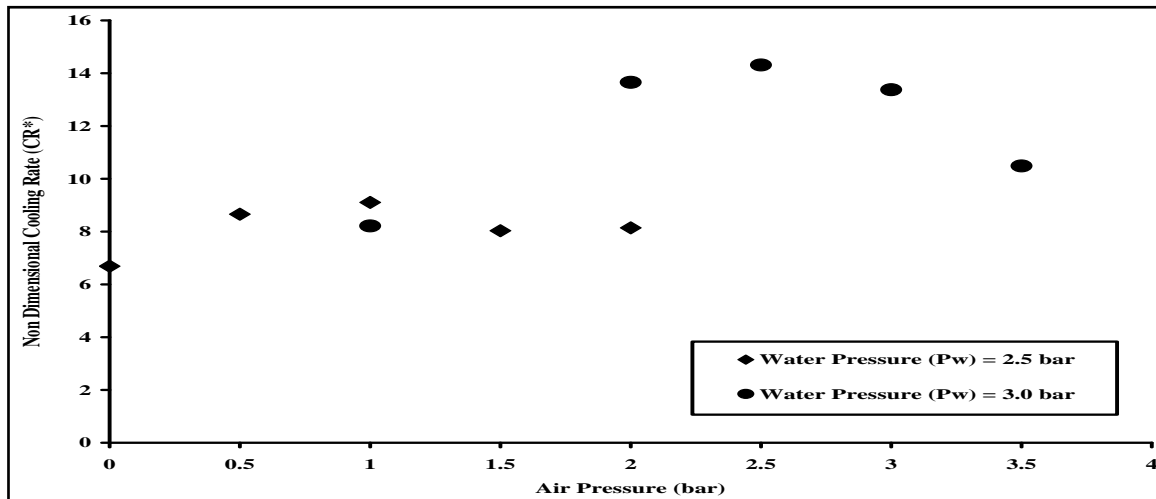


Figure- 5. Air Pressure Vs. Non Dimensional Cooling Rate (CR\*) At Tc3 (Central Thermocouple) For Different Fixed Water Pressures

As the pressure of the cooling water increased at a constant air pressure, the flow rate of the water increased. The mass flow ratio increased with increasing water pressure or decreasing air pressure.

**4.4. Effect of Water Flow Rate:**

Figures 6 represent the effect of water flow rates to the dimensionless cooling rates at the location of central thermocouple on the steel plate surface for different water pressure values. From Figure 6, it could be observed that, there was no definite trend between cooling rate and water flow rate. This was because of the fact that in this case cooling was caused both by air flow and water spray. The contribution of both air and water were significant and responsible for cooling effect. Hence water flow rate alone cannot be used to improve the cooling rate. High flow rate in a spray quench accelerates cooling but there still exists the “limit” of the cooling rate in each specific operating condition. The nature of the distribution shows that an optimal value of the dimensionless cooling rate exists. The optimal value of cooling rate can be obtained through optimisation of water flow rate, i.e., optimising the air-water pressure values. The low was the air pressure, the higher water flow rate achieved and less atomization appeared. Whereas, for the very high values of air pressure, the water flow rate values were low and atomization was high. From Figure 6, it is clear that for higher value of water pressure (Pw), the cooling rate was enhanced. In one set of experiments, for a fixed water pressure of 2.5 bar and variation of water flow rate from 300 LPH to 500 LPH, the highest non dimensional cooling rate (CR\*) achieved at the centrally place thermocouple was ranged from 6.68 to 9.1.

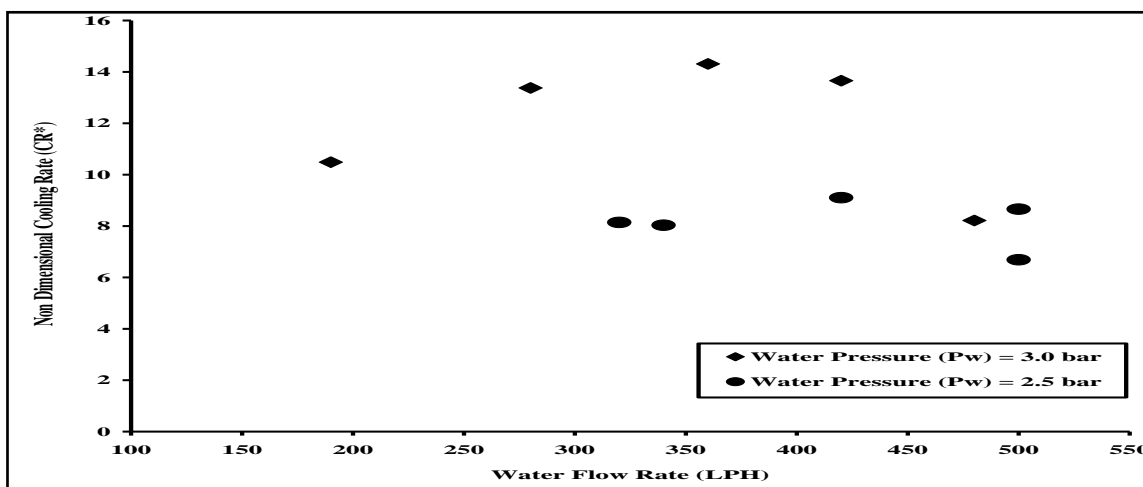


Figure 6: Water Flow Rate (Wfr) Vs. Non Dimensional Cooling Rate (CR\*) At Central Thermocouple (Tc3) For Different Water Pressures (Pw).

While, in the other set of experiments, with 3.0 water pressure and water flow rate in the range of 190 LPH to 420 LPH, the non dimensional cooling rate ( $CR^*$ ) obtained was in the range of 10.4 to 13.6. Hence, it can be predicted that the optimal value of cooling rate could be achieved by optimizing the water flow rate during spray cooling through appropriate combination of air and water pressure values.

**4.5. Mass Impingement Density :**

The liquid mass flux plays major role in metal quenching applications, especially in the heat transfer characteristics investigations during spray cooling. A simple mechanical patternator, the liquid mass flux (or liquid impingement density) was measured at various combinations of the air and water pressures. The local impingement density values were plotted against the tube distances in Figures 7. The measurements were at a constant water pressure and varying air pressure for all the three air atomizing nozzles.

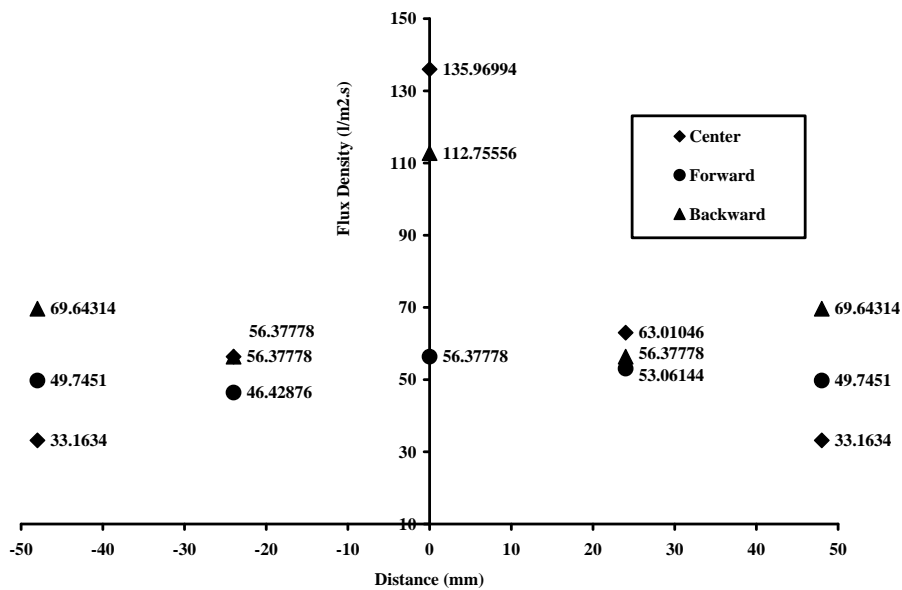


Figure- 7: Local Impingement Density vs. Tube Distance.

It can be seen from above Figures 7 that a bell-shaped profile results with a maximum impingement density at the center of the spray. For constant water flow and increasing air pressure the maximum impingement density decreases. This is because of the fact that at higher air pressure, smaller drops were formed, which followed the airflow better and were thus more dispersed. This led to reduction in impingement density at the plate center. All the results were obtained at three locations, i.e., at the center of the nozzle bank, 15 mm forward and 15 mm backward positions.

**1.6. Effect of Spray Impingement Density on Heat Transfer:**

Figure 8 presents the data of non-dimensional cooling rate with respect to mean spray density and standard deviation spray density, which show a very clear trend of increasing with mass flux. At low values of mean spray density, this non-dimensional cooling rate is higher for the vertical down spray. Also, at low mean spray density values, the non-dimensional cooling rate at the center location are higher than that at the side location of a downward spray. These observations of orientation and angle of attack effects do not appear in high spray density tests, since the spray impingement is the dominant factor. The cooling characteristics can be well understood by statistical analysis of cooling data.

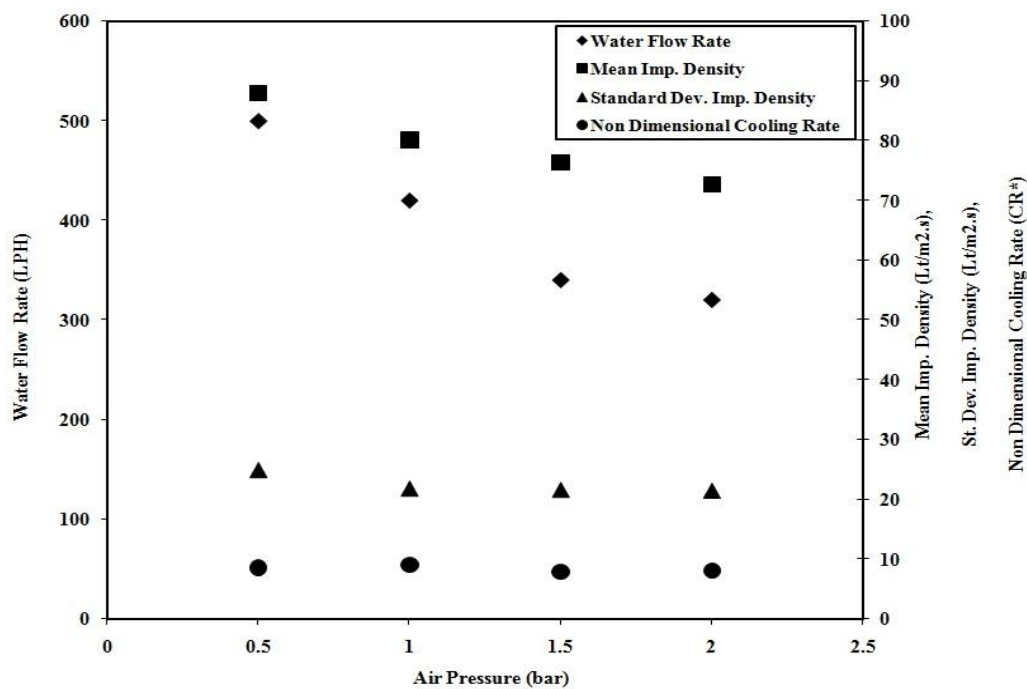


Figure 8. Cooling Rate Versus Spray Impingement Density At Fixed Water Pressure = 2.5 Bar.

## V. CONCLUSION

A transient method was used for investigating the heat transfer characteristics of atomized air-water spray impingement cooling of flat steel plate with application to the design of impingement cooling facility. Air-water spray impingement cooling was found as an efficient alternative cooling technique over the conventional laminar water jet impingement cooling to achieve the optimal and very high cooling rate. Air assisted double distilled water was chosen as the quenchant. The heat transfer distribution was measured from a multi-droplet array of liquid at varied range of spray flux density.

The heat transfer phenomena of this atomized air-water spray impingement cooling systems, which have been demonstrated, are as follows:

1. The surface temperature profiles provided a better understanding of impingement heat transfer during quenching of high hot steel plate. They also provided more insight for parametric analysis.
2. It is possible to obtain the very high strip cooling rate in a 4 mm thick steel strip by spray impingement cooling provided very small droplet size. These results have a good agreement with the results obtained analytically by Bhattacharya et al. [6].
3. With the variation of air-to-water mass flow ratio, the value of dimensionless cooling rate ( $CR_{max}^*$ ) accordingly changed but the consistent variation tendencies against either the increase of airflow rate or water flow rate are not found. The optimal selection of water flow ratio of a spray impinging jet for obtaining the maximum heat transfer value thus depends on the airflow rate.
4. For a fixed water pressure and varying air pressure, the cooling rate increases with increase in air pressure at the fixed water pressure.
5. At different combinations of air and water pressures, the higher cooling rate was achieved at the centrally located thermocouple where the local impingement density was maximum.
6. The present cooling technique was found greatly advantageous because, due to contributory effect of air present in the mixture the water consumption was very less and effectively high cooling rate was achievable for Spray cooling.
7. It is believed that at higher spray density, the effect of droplet size or orientation on heat transfer is minimal. The droplet velocity, on the other hand, may have important effect.



## REFERENCES

- [1] Selvam, R.P., Lin, L., Ponnappan, R. "Direct simulation of spray cooling: Effect of vapor bubble growth and liquid droplet impact on heat transfer". *Int. J. Heat Mass Transfer* (49) , 2006 , pp- 4265-4278.
- [2] Lucas, A., Simon, P., Bourdon, G., Herman, J.C., Riche, P., Neutjens, J., Harlet, P. "Metallurgical aspects of ultra fast cooling in front of the down-coiler", *Steel Research* 75 (2), 2004, pp- 139-146.
- [3] Herman, J.C. "Impact of new rolling and cooling technologies on thermo-mechanically processed steels", *Ironmaking & Steelmaking* 28 (2), 2001, pp- 159-163.
- [4] Akio, F. and Kazuo, O. *JFE Technical Report*(5), 2005, pp. 10–15 .
- [5] Akio, F., Sadanori, I., Yoshimich, H. Toru, M., Yoichi, M., and Shozo, I . EP Patent Application, 2002, EP1210 993 A (1).
- [6] Bhattacharya, P., Samanta, A. N., Chakraborty, S . "Spray evaporative cooling to achieve ultra fast cooling in runout table", *Int. Journal of Thermal Sciences*, 2009, pp- 1–7.
- [7] Buyevich, Y.A., and Mankevich, V.N. *Int. J. Heat Mass Transfer*, vol. 38, 1995, pp. 731–44.
- [8] Yao, S.C., and Cai, K.Y. *Exp. Therm. Fluid Sci.*, vol. 1, 1988, pp. 363–71.
- [9] Jenkins, M.S., Story, S.R., and David, R.H . *Proc. 19th Australasian Chem. Eng. Conf., CHEMECA 91*, Newcastle, New South Wales, Australia, Sept. 12–20, Institute of Chemical Engineers, North Melbourne, 1991.
- [10] Satya V. Ravikumar , Jay M. Jha , Ishita Sarkar , Soumya S. Mohapatra , Surjya K. Pal , Sudipto Chakraborty . "Achievement of ultrafast cooling rate in a hot steel plate by air-atomized spray with different surfactant additives". *Experimental Thermal and Fluid Science* (50), 2013, pp-79–89.
- [11] Yu Houa, Xiufang Liu , Jionghui Liu , Mengjing Li , Liang Pu . "Experimental study on phase change spray cooling". *Experimental Thermal and Fluid Science* (46 ) , 2013, pp-84–88.
- [12] Zhen Zhang , Jia Li , Pei-Xue Jiang . "Experimental investigation of spray cooling on flat and enhanced surfaces". *Applied Thermal Engineering* (51) , 2013, 102e111 .
- [13] 1.J. Wendelstorf \*, K.-H. Spitzer, R. Wendelstorf , Spray water cooling heat transfer at high temperatures and liquid mass fluxes, *International Journal of Heat and Mass Transfer* 51 , 2008, 4902–4910 .